J Nanostruct 16(3): 3972-3980, Summer 2026

RESEARCH PAPER

Tuning the Crystal Structure and Optoelectrical Properties of Cu_2ZnSnS_4 Thin Film Nanocomposites via Partial Substitution of Zn^{2+} with Fe^{3+}

Fadhel H. Ali [1], Lara A. Kzar [2], Bashaer J. Kahdum [3]*

[1] *Department of Physics, College of Science, University of Babylon, Babylon, Iraq*
[2] *Department of Chemical Engineering, Faculty of Engineering, University of Kufa, Najaf, Iraq*
[3] *Geomatics Technology Center, University of Kufa, Najaf, Iraq*

ARTICLE INFO

Article History:
Received 20 April 2026
Accepted 22 June 2026
Published 01 July 2026

Keywords:
Cu_2ZnSnS_4 thin film
Optical properties
Photovoltaic applications
Solvothermal method
Spin coating

ABSTRACT

In this report, Cu_2ZnSnS_4 and $Cu_2Zn_{0.5}Fe_{0.5}SnS_4$ thin films were produced using the solvothermal method followed by spin-coating. The effect of partial doping of Zn^{2+} with Fe^{3+} on the structural, morphological, and optoelectrical properties was investigated. The XRD results have shown that both films consist of pure kesterite structure without clear secondary phases, with a slight change in the lattice constants and crystallite size due to the introduction of Fe. The EDS analysis confirmed the success of the doping process through the reduction in Zn concentration and the presence of Fe in proportions, the samples were transformed into a Cu-Poor and S-rich condition, which is an ideal combination to improve optoelectrical properties. FESEM images have shown that films had a homogeneous and dense surface, where the film's thickness was decreased from 2.07μm to 1.24μm in the Cu_2ZnSnS_4 and $Cu_2Zn_{0.5}Fe_{0.5}SnS_4$ thin films respectively, which reflects the effect of Fe incorporation. From an optical-electric perspective, UV-Visible spectra revealed the increase in absorption coefficients and refraction index, as well as an increase in optical conductivity and continuous increase in extinction coefficient. Under the lights in the I-V curve also improvement in photoelectric reaction, with increasing photosensitivity from 16.21% in the Cu_2ZnSnS_4 thin film to 18.67% in the $Cu_2Zn_{0.5}Fe_{0.5}SnS_4$ thin film. These results confirm that the introduction of Fe^{3+} at the Zn^{2+} site is an effective strategy for setting the structure and improving optoelectrical properties, making the $Cu_2Zn_{0.5}Fe_{0.5}SnS_4$ thin film a promising candidate in thin film Solar cells and photovoltaic systems.

How to cite this article
Ali F., Kzar L., Kahdum B. Tuning the Crystal Structure and Optoelectrical Properties of Cu_2ZnSnS_4 Thin Film Nanocomposites via Partial Substitution of Zn^{2+} with Fe^{3+}. J Nanostruct, 2026; 16(3):3972-3980. DOI: 10.22052/JNS.2026.03.081

INTRODUCTION

Global interest in renewable energy sources has increased in recent decades due to environmental challenges such as climate change and the gradual depletion of fossil fuels, which has prompted researchers to develop advanced materials for photovoltaic conversion technologies [1]. Thin-film solar cells are among the promising solutions

* *Corresponding Author Email: sci.fadhel.hasan@uobabylon.edu.iq*

that combine low cost with high potential for widespread application as their small thickness, light weight, and ability to be deposited on flexible substrates [2]. Within this category, Cu_2ZnSnS_4 (CZTS) has emerged as one of the most important p-type chalcopyrite semiconductors, with outstanding physical and photovoltaic properties that make it a strong candidate for next-generation solar cell technologies. On the one hand, CZTS has a direct bandgap located in the ideal range (1.4–1.6 eV), which corresponds to the ideal absorption window for sunlight. On the other hand, the compound has a high absorption coefficient (>10^4 cm^{-1}), allowing most of the visible solar radiation to be absorbed in relatively thin layers of only a few micrometres [3]. In addition, the component elements (Cu, Zn, Sn and S) are plentiful in nature and are relatively non-types compared to other compounds used in solar cells such as CdTe and CIGS, which increases the environment and economic stability [4]. Despite these benefits, the CZTS crystal structure encounters is some restrictions that limit its final efficiency in photovoltaic applications. The most remarkable crystalline defects in these boundaries that Cu_{Zn} and Zn_{Cu} form, leading to non-conversion regenerations of photo-carriers, thus reducing the output voltage (V_{OC}) [5]. The narrow chemical composition of CZTS also sometimes leads to the presence of unwanted secondary phases such as Cu_2SnS_3 and ZnS, which adversely affects optical and electrical properties [6]. For this reason, several recent studies have used improvement strategies that include doping or ionic replacement to control the crystal structure and reduce the effect of defects. In this context, the introduction of divalent or trivalent metal elements at various sites in the crystal lattice is an effective way to modify the electronic and optical properties of the compound. The effect of doping with elements such as Co, Ni, Mn, and Ag has been studied, and the results have shown the possibility of tuning the band gap and improving electrical conductivity [7, 8]. However, studies on the use of iron Fe^{3+} as a partial substitute for zinc Zn^{2+} are still relatively limited, although this type of substitution holds great potential. This is because Fe^{3+} has an ionic radius close to that of Zn^{2+} (0.64Å versus 0.74Å), which facilitates its incorporation into the crystal lattice without causing significant distortions [9]. In addition, the trivalent valence of iron can induce a redistribution in the density of electronic states, which may be reflected in improved light absorption and the generation of additional photo-carriers [10].

MATERIALS AND METHODS

Synthesizing and Preparation methods (solvothermal and spin coating)

The solvothermal synthesis method was used to prepare the compound Cu2ZnSnS4 (CZTS). 0.2 g of $CuCl_2$ dehydrate ($2H_2O$), 0.1 g of $ZnCl_2$, and 0.15 g of $SnCl_2$ pentahydrate ($5H_2O$) were dissolved in 40 mL of ethylene glycol as the solvent, with continuous magnetic stirring at room temperature for 30 minutes to ensure complete dissolution and homogeneity of the solution. Subsequently, 0.4 g of thiourea ($SC(NH_2)_2$) was added to the mixture as a sulfur source, with continued stirring until a dark, homogeneous solution was obtained. The solution was then transferred to a Teflon-lined autoclave (50 mL capacity) and incubated at 220°C for 15 hours. After the reaction was completed, it was allowed to gradually cool to room temperature. The resulting precipitate was collected by filtration and washed several times with a mixture of distilled water and ethanol to remove any unreacted impurities. Finally, it was dried in an oven at 70°C for 6h to obtain pure CZTS powder. In the case of $Cu_2Zn_{0.5}Fe_{0.5}SnS_4$ partial replacement of zinc was carried out by adding 0.05g of $FeCl_3$ $6H_2O$ to replace a portion of the previous zinc chloride, while maintaining the remaining reaction conditions. To prepare the thin films, 0.3g of pure CZTS powder (iron-doped) was first dissolved in a 10mL of absolute ethanol with two drops of PVA added as a binder to improve the viscosity of the solution. Drops of the solution were placed onto clean microscopic glass substrates and then spread using a spin coater at 2500 rpm for 45s to obtain a homogeneous layer. After each layer, the samples were dried on a hot plate at 120°C for 10min to evaporate the solvent. The process was repeated four times to obtain a suitable film thickness. Finally, an annealing process was performed at 350°C for 1h in a sulfur-saturated argon (Ar) atmosphere to improve crystallinity and increase phase purity. Thus, homogeneous and well-adhered CZTS and Fe-CZTS thin films were obtained, ready for structural, optical and electrical investigations.

Characterization

To achieve a comprehensive evaluation of the

prepared samples, a set of advanced analytical techniques was adopted. To study the crystal structure and determine the crystalline phase of the compound, X-ray diffraction (XRD) was used. Field-emission scanning electron microscopy (FESEM) was employed to analyze the topographic properties of the thin films, examine their cross-sections, and precisely analyze their elemental composition and confirm the proportions of the constituent elements. UV-visible spectroscopy was used to study the optical properties, determine the light absorption behaviour, and assess the spectral characteristics of the samples. Finally, current-voltage (I-V) curves were measured to evaluate the electrical properties and their correlation with the crystal structure and nanoparticle shape.

RESULTS AND DISCUSSION

Crystal structure properties

Fig. 1 shows distinct peaks at (112), (220), and (132) of the X-ray diffraction (XRD) patterns of the prepared films, which correspond well to the tetragonal kesterite phase of CZTS. This confirms the formation of the desired main phase without the appearance of distinct, high-intensity secondary peaks. A slight shift of the (112) peak from 28.527° to 28.594° was observed upon the addition of iron, accompanied by a decrease in the inter-plane distance from 3.1264 to 3.1211 Å. This shift is attributed to the introduction of Fe^{3+} ions with a smaller ionic radius compared to Zn^{2+} ions, causing localized changes in the crystal lattice and a relative shrinkage in some crystallographic directions, in accordance with Bragg's law [11].

Furthermore, as summarized in Table 1, the lattice constants calculations showed an increase in "*a*" from 5.4169 to 5.5399 Å, with a clear decrease in "*c*" from 10.8231 to 10.3294 Å, while the unit volume remained almost constant (317.58 → 317.01 $Å^3$). This anisotropic behavior reflects internal ion rearrangements, vacancy formation, or cation disorder between Cu/Zn/Fe to compensate for the charge difference between Zn^{2+} and Fe^{3+}, as previously reported in similar studies on the effect of Zn substitution with transition elements in the kesterite structure [12,13]. In addition, a slight increase in crystalline size indicates from 6,418 to 6,742 nm, with a slight reduction in microstrain, a

Table 1. Crystal structure parameters of Cu_2ZnSnS_4 and $Cu_2Zn_{0.5}Fe_{0.5}SnS_4$ thin films.

Thin films	Cu_2ZnSnS_4	$Cu_2Zn_{0.5}Fe_{0.5}SnS_4$
Diffraction dominant peak 2θ (°)	28.527	28.594
d-spacing (Å)	3.1264	3.1211
Lattice constants "*a*, *c*" (Å)	*a* = 5.4169 *c* = 10.8231	*a* = 5.5399 *c* = 10.3294
c/a	1.9980	1.8645
$V=a^2c$ ($Å^3$)	317.58	317.01
η=c/2a	0.9990	0.9323
Crystallite Size only (nm)	6.418	6.742
Micro Strain (%)	0.0219	0.0208

limited improvement in crystal development and a reduction in internal defects due to doping [14]. Therefore, it can be observed that the introduction of Fe^{3+} at a ratio of (x=0.5) did not cause a radical change in the main crystal phase, but it did lead to a significant anisotropic distortion in the crystal lattice, with the potential generation of vacancies and ionic exchanges. These structural changes are expected to directly affect the optical and electronic properties of the thin films, especially with regard to the energy gap and photo carrier behavior [13,15]. XRD results confirm that adding iron at a Zn:Fe ratio of 0.5 does not alter the main crystalline phase of Cu_2ZnSnS_4 it remains generally conserved. However, changes in the lattice constants and complex ionic distribution, along with charge compensation and a slight increase in crystal size, are observed, accompanied by a decrease in micro-stress, indicating relative stability and a minor crystalline improvement. These structural changes may affect the electronic and optical properties of the films, including energy differences, charge carrier behavior, and defects.

Elemental composition

EDS analysis was done to confirm their basic creation both Cu_2ZnSnS_4 and $Cu_2Zn_{0.5}Fe_{0.5}SnS_4$ thin films and confirm the success of partial doping of Fe in the Zn replacement. As shown in Fig. 2, spectra showed the presence of characteristic peaks for Cu, Zn, Sn and S elements in Cu_2ZnSnS_4 thin film, while an additional Fe peak appeared in the $Cu_2Zn_{0.5}Fe_{0.5}SnS_4$ thin film, confirming that the substitution had indeed occurred. Quantitatively, the Zn content dropped from 7.34% to 2.39%, with Fe 4.13%, while the copper content was close to its original value. There was also a small increase in Sn and a slight reduction in sulfur, including S/(Cu+Zn+Sn+Fe) ratio remains close to unit, indicating that films are still a bit sulfur -rich. The Cu/(Zn+Sn+Fe) ratio dropped from 0.770 to 0.706, resulting in different conditions (Cu-poor and S-rich) reducing the formation of secondary phases

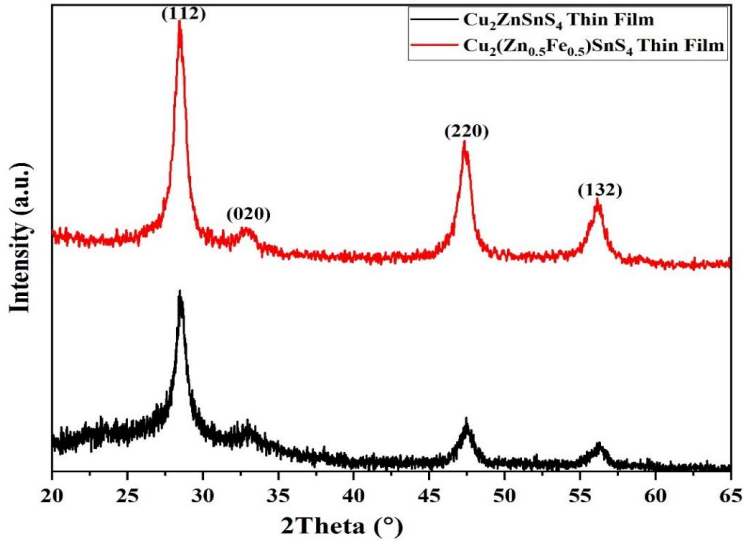

Fig. 1. XRD pattern of the Cu_2ZnSnS_4 and $Cu_2Zn_{0.5}Fe_{0.5}SnS_4$ thin films.

Table 2. The elemental ratio of the Cu_2ZnSnS_4 and $Cu_2Zn_{0.5}Fe_{0.5}SnS_4$ thin films.

Thin films	Cu%	Zn%	Fe%	Sn%	S%	Cu/(Zn+Sn+Fe)	S/(Cu+Zn+Sn+Fe)
Cu_2ZnSnS_4	24.14	7.34	0	24.2	44.32	0.770	0.796
$Cu_2Zn_{0.5}Fe_{0.5}SnS_4$	23.29	2.39	4.13	26.46	43.73	0.706	0.777

such as Cu_2S and Cu_2SnS_3 and to improve electron transport properties to thin-film solar cells. These results correspond to previous literature reporting that compensation with infection metals that Fe can significantly change the chemical composition, which affects the electronic and optical properties of the compound [12,16,17]. Depending on the EDS results, partial doping of Zn with Fe was clearly achieved, as the Fe peak and a low Zn content were detected.

The films also maintained the overall kesterite composition with slight deviations in the Sn and S ratios. The transition of the samples towards a Cu-poor and S-rich state is a positive indicator of improved structural stability and reduced secondary phases, which will be reflected in the future enhancement of the electronic and optical properties of the films.

Topographical analysis

As shown in the Fig. 3, FESEM images of Cu_2ZnSnS_4 and $Cu_2Zn_{0.5}Fe_{0.5}SnS_4$ thin films showed distinct differences in topographical properties. In the thin film Cu_2ZnSnS_4, the surface appeared

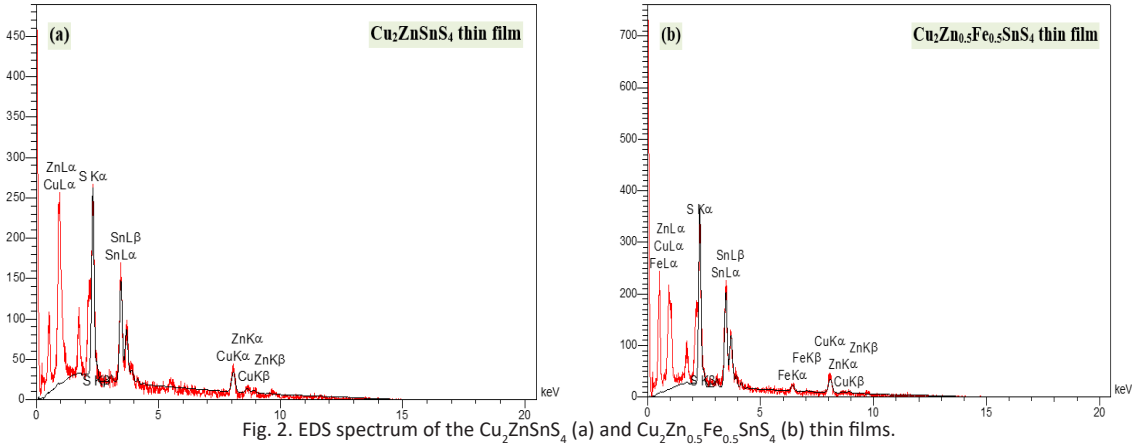

Fig. 2. EDS spectrum of the Cu_2ZnSnS_4 (a) and $Cu_2Zn_{0.5}Fe_{0.5}SnS_4$ (b) thin films.

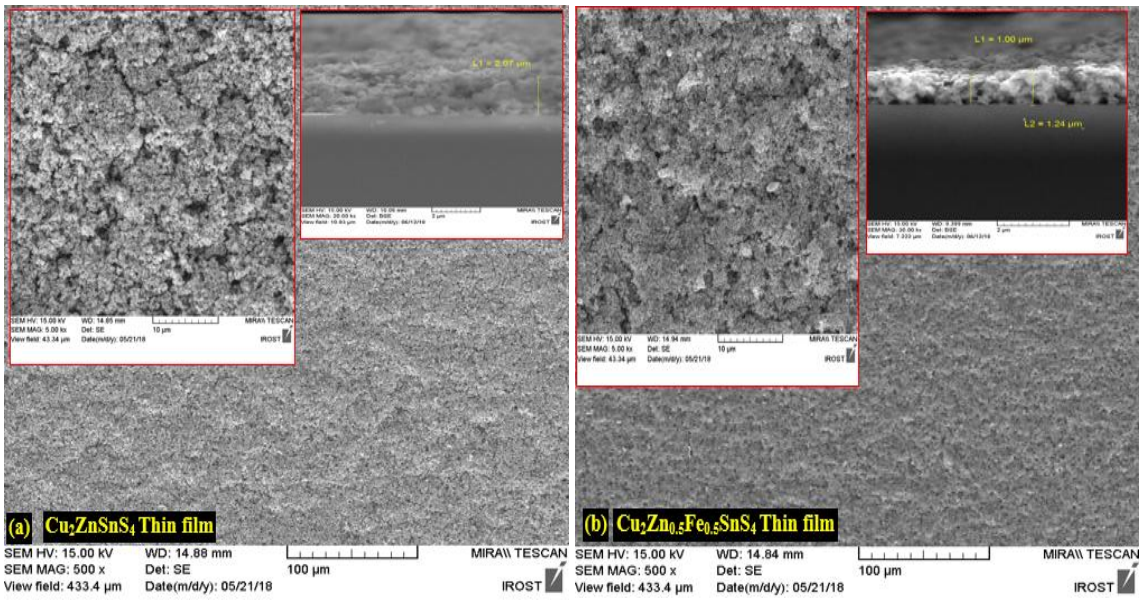

Fig. 3. FESEM images of the Cu_2ZnSnS_4 (a) and $Cu_2Zn_{0.5}Fe_{0.5}SnS_4$ (b) thin films.

granulated with clear agglomerated and strange grain distribution, as well as some fine interstitial voids. The cross -sectional scene showed that the thickness of the film was around 2.07µm, but the structure was not completely compact. In contrast, the $Cu_2Zn_{0.5}Fe_{0.5}SnS_4$ thin film performed a more homogeneous surface with fine and low agglomerate grain, and the structure seemed more compact as the thickness was reduced to about 1.24µm. The morphological improvement resulting from iron doping contributes to controlling grain growth and reducing defect density, leading to a more homogeneous and stable layer [18, 19]. Previous reports also indicate that adding metals such as iron, chromium, or bismuth can significantly improve the thin-layer surface structure and stability, which in turn affects its optical and photonic properties by reducing bonding centres and increasing light absorption [19-22]. FESEM images show that the surface of the Cu_2ZnSnS_4 composite thin film is relatively homogeneous with a uniform grain distribution, while the iron-doped sample exhibits smaller grain size and increased fragmentation, indicating that the iron element modifies the layer morphology and reduces its thickness from 2.07 to 1.24µm. These morphological changes may directly affect the optical properties of the material, which is an important indicator for understanding its behaviour in solar and photovoltaic applications.

Optoelectrical properties

Spectroscopic measurements showed that the introduction of Fe into Cu_2ZnSnS_4 resulted in a slight change in the absorption coefficient and optical properties. As shown in the Fig. 4, although the doped sample was thinner, it exhibited lower transmittance and higher absorption coefficients, indicating an expanded role for defect states or intermediate levels resulting from the substitution of Zn by Fe. These changes are consistent with the XRD, EDS, and FESEM results, which indicate local charge compensation and modified grain growth. They predict two opposing effects on device performance: enhanced light absorption on the one hand, and increased potential re-bonding centers on the other [15]. The introduction of Fe did not radically change the overall absorption, but it did introduce slight changes in the density of defect states or in transitions near the band edge. This is consistent with a slight change in crystal structure and the presence of charge compensation [16]. Although the $Cu_2Zn_{0.5}Fe_{0.5}SnS_4$ thin film is thinner, its transmittance is lower-indicating that the transmittance reduction is not due solely to thickness, but rather to increased intrinsic absorption or scattering caused by defect states or additional energy levels by Fe. In other words, Fe increases the material's absorbance per unit thickness, which corresponds to the appearance of defect states at the center of the beam that absorb light and reduce transmittance. As shown in the Fig. 5, extinction coefficient represents a portion of the complex refractive index and is directly related to the loss of optical energy within the material (absorption). It appears higher or

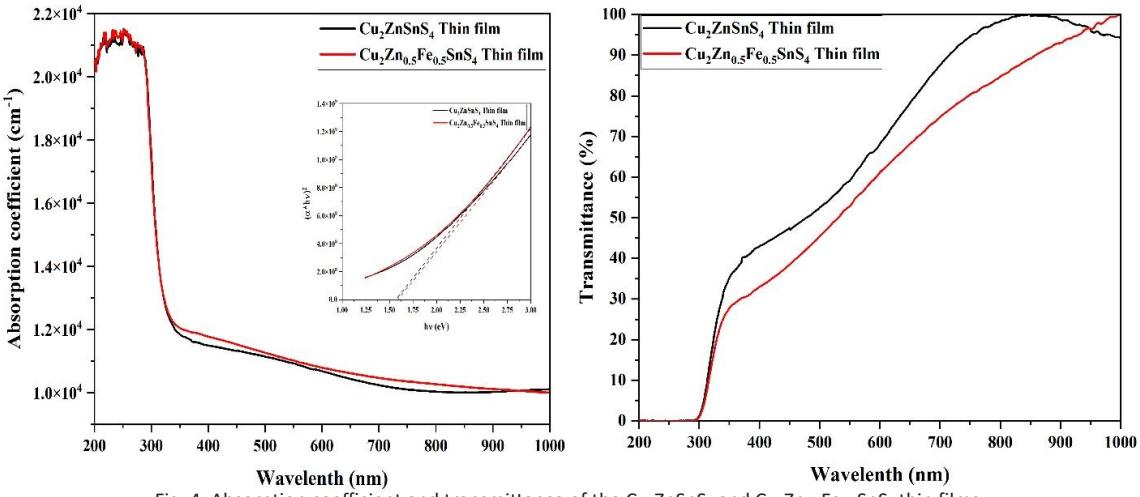

Fig. 4. Absorption coefficient and transmittance of the Cu_2ZnSnS_4 and $Cu_2Zn_{0.5}Fe_{0.5}SnS_4$ thin films.

similar to the doped sample at wavelengths near UV/Visible, supporting the hypothesis of the presence of additional absorption

centers (defect-related absorption) when Fe is added. Higher extinction coefficient near the energy edge indicates an increased probability of optical transitions through moderate sub-bandgap states, which may be due to Fe or associated vacancies (V_{Cu}).

The $Cu_2Zn_{0.5}Fe_{0.5}SnS_4$ thin film exhibits a higher peak in optical conductivity around the same energy edge range (300–400 nm) compared to the Cu_2ZnSnS_4 thin film followed by a gradual decline. This indicates an increase in the material's response to the photo-electromagnetic field most likely a result of increased carrier density, increased photo-transmission through defect states, or increased electronic polarization at certain frequencies. This suggests that Fe increases the material's ability to conduct an optical signal due to carriers or intermediate states, although this may be accompanied by increased charge loss (recombination). In general, increasing light absorption near the edge may be beneficial for capturing more photons, but if this is accompanied by a higher number of recombining centers, it will reduce the open-circuit voltage (V_{OC}) and the conversion efficiency. Therefore, a balance is required: improving absorption while reducing defect centers [12,17,19]. The Fig. 6, shows that the refractive index (n) values for the Cu_2ZnSnS_4 thin film rise rapidly at short wavelengths from 300nm to 400nm, reaching a peak around 9, and then gradually decrease. When doped with iron ($Cu_2Zn_{0.5}Fe_{0.5}SnS_4$ thin film), it was observed higher n values across almost the entire spectral range, reaching a peak of about 11 at wavelength about 330nm. This increase

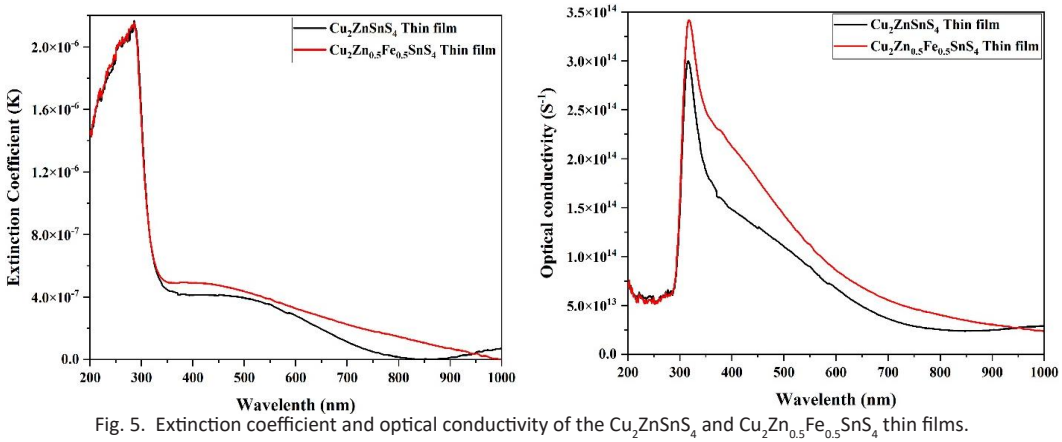

Fig. 5. Extinction coefficient and optical conductivity of the Cu_2ZnSnS_4 and $Cu_2Zn_{0.5}Fe_{0.5}SnS_4$ thin films.

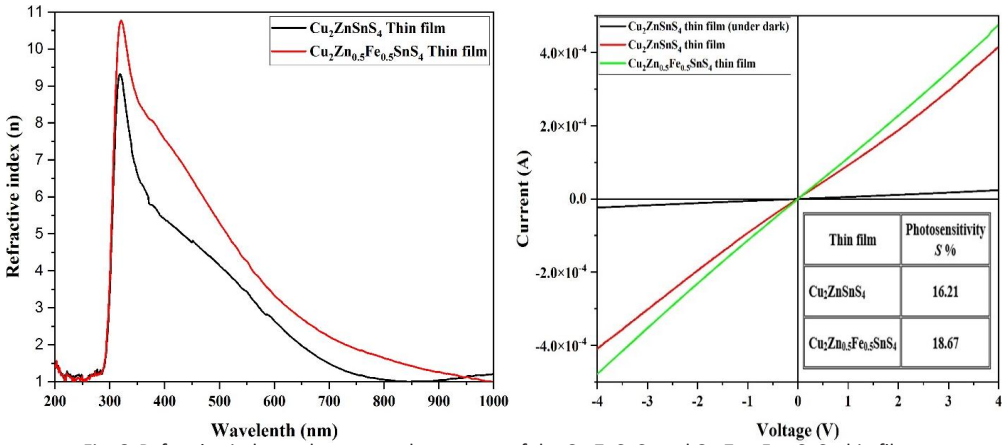

Fig. 6. Refractive index and current-voltage curve of the Cu_2ZnSnS_4 and $Cu_2Zn_{0.5}Fe_{0.5}SnS_4$ thin films.

is explained by the fact that Fe doping leads to an increased density of electronic states in the conduction band or valence band, which enhances the polarization of light within the material and increases the interaction between photons and electrons [23]. This result is important for thin film solar cell application, as a higher n at UV-Visible wavelengths means stronger light absorption, thus improving photovoltaic conversion efficiency [24]. The current-voltage (I-V) figure shows that both thin films exhibit near-linear behavior, with a significant difference between measurements under dark and illuminated conditions. For the Cu_2ZnSnS_4 thin film the photosensitivity S = 16.21%, while the value increased to 18.67% for the $Cu_2Zn_{0.5}Fe_{0.5}SnS_4$ thin film.

This clearly indicates that the introduction of Fe improves the film's photosensitivity by reducing recombination centers or modifying defect levels, improving electron transport and increasing the concentration of photo-generated carriers and enhancing photoconductivity due to improved electron-hole balance [25].

Overall, it is clear that the partial doping of Fe in the Cu_2ZnSnS_4 structure significantly improves optoelectrical properties. The increased refractive index at short wavelengths enhances the light absorbance and photon harvesting efficiency, which is directly reflected in the current response under illumination. The correlation between the increased n and the better I-V curve shows that the introduction of Fe increases photo- carrier transport by improving optical reaction and reducing certain electrical obstacles. Therefore, it can be argued that iron doping Cu_2ZnSnS_4 provides a promising passage to set the optoelectrical properties of the thin film, which constitutes the ability for a more effective application of these materials in solar cells with thin films and future photovoltaic conversion devices.

CONCLUSION

This study demonstrated that the $Cu_2Zn_{0.5}Fe_{0.5}SnS_4$ thin film represents an effective film with structural and optoelectrical properties suitable for photovoltaic applications. The results revealed that partial doping of Zn^{2+} with Fe^{3+} significantly improved the properties, contributing to fine-tuning the crystal structure without the formation of secondary phases. Partial replacement affected the topographic properties of a thin film, which directly affected the light absorption properties. In addition, the absorption and refraction index increased, improved optical conductivity and improved photoelectric response. Therefore, it can be argued that introducing Fe^{3+} at the Zn^{2+} site in the Cu_2ZnSnS_4 thin film is an effective strategy to improve the performance of the thin film, making it a promising candidate in solar cells and sustainable photovoltaic conversion systems.

ACKNOWLEDGEMENTS

The authors thank the University of Kufa for providing laboratory support.

CONFLICT OF INTEREST

The authors declare that there is no conflict of interests regarding the publication of this manuscript.

REFERENCES

1. Younus NC, Hussein HM. A competitive candidate for the Cu_2ZnSnS_4 compound in solar photocatalytic degradation of organic pollutants. AIMS Materials Science. 2025;12(2):380-394.
2. Ajeel FN, AlGelal HMAA, Hamza LA, Ziadan KM, Al-Kabbi AS, Hussein HM, et al. I-V characteristic of tri ethanol amine capped CdSe thin films. AIP Conference Proceedings: AIP Publishing; 2023. p. 050015.
3. Shockley W, Queisser H. Detailed Balance Limit of Efficiency of p–n Junction Solar Cells. Renewable Energy: Routledge; 2018. p. 35-54.
4. Mitzi DB, Gunawan O, Todorov TK, Wang K, Guha S. The path towards a high-performance solution-processed kesterite solar cell. Sol Energy Mater Sol Cells. 2011;95(6):1421-1436.
5. Ali FH, Naser BA. Non-linear optical properties for mixture of Rhodamine B and methyl violet 10 B laser dyes. AIP Conference Proceedings: AIP Publishing; 2023. p. 090053.
6. Fernandes PA, Salomé PMP, da Cunha AF. Growth and Raman scattering characterization of Cu_2ZnSnS_4 thin films. Thin Solid Films. 2009;517(7):2519-2523.
7. Syafiq U, Ataollahi N, Maggio RD, Scardi P. Solution-Based Synthesis and Characterization of Cu_2ZnSnS_4 (CZTS) Thin Films. Molecules. 2019;24(19):3454.
8. Yang X, Qin X, Yan W, Zhang C, Zhang D. Effects of Mn and Co Doping on the Electronic Structure and Optical Properties of Cu_2ZnSnS_4. Crystals. 2025;15(9):781.
9. Shannon RD. Revised effective ionic radii and systematic studies of interatomic distances in halides and chalcogenides. Acta Crystallographica Section A. 1976;32(5):751-767.
10. Wang W, Winkler MT, Gunawan O, Gokmen T, Todorov TK, Zhu Y, et al. Device Characteristics of CZTSSe Thin-Film Solar Cells with 12.6% Efficiency. Advanced Energy Materials. 2013;4(7).
11. Ali FH, Naser BA. Non-linear optical properties of malachite green dye. AIP Conference Proceedings: AIP Publishing; 2023. p. 090047.
12. Schorr S. The crystal structure of kesterite type compounds: A neutron and X-ray diffraction study. Sol Energy Mater Sol

Cells. 2011;95(6):1482-1488.
13. Valdés M, Di Iorio Y, Castañeda K, Marotti RE, Vázquez M. Cu_2ZnSnS_4 thin films prepared by sulfurization of co-electrodeposited metallic precursors. J Appl Electrochem. 2017;47(6):755-765.
14. Aldakov D, Lefrançois A, Reiss P. Ternary and quaternary metal chalcogenide nanocrystals: synthesis, properties and applications. Journal of Materials Chemistry C. 2013;1(24):3756.
15. Chen S, Yang J-H, Gong XG, Walsh A, Wei S-H. Intrinsic point defects and complexes in the quaternary kesterite semiconductor Cu_2ZnSnS_4. Physical Review B. 2010;81(24).
16. Chen M-M, Xue H-G, Guo S-P. Multinary metal chalcogenides with tetrahedral structures for second-order nonlinear optical, photocatalytic, and photovoltaic applications. Coord Chem Rev. 2018;368:115-133.
17. Burton LA, Colombara D, Abellon RD, Grozema FC, Peter LM, Savenije TJ, et al. Synthesis, Characterization, and Electronic Structure of Single-Crystal SnS, Sn_2S_3, and SnS_2. Chem Mater. 2013;25(24):4908-4916.
18. Shariful I, Payal M, Md. Abul H, Farid A. Effect of Fe^{3+} Doping Concentration in Cu_2ZnSnS_4 Thin Film: Structural and Optical Analysis. Journal of Materials Science and Engineering A. 2022;12(3).
19. Hussein H, Yazdani A. Investigation the influence of Fe (III) doping in Cu_2ZnSnS_4 semiconductor: Structural, optical and magnetic properties. Optik. 2019;179:505-513.
20. Hussein H, Yazdani A. Spin-coated Cu_2CrSnS_4 thin film: A potential candidate for thin film solar cells. Mater Sci Semicond Process. 2019;91:58-65.
21. Hussein HM, Sharifi S, Yazdani A. Effect of substituting the ionic radius in the structural and optoelectrical properties of spin-coated thin film synthesized by solvothermal method. Optik. 2021;241:166975.
22. Hussein H, Yazdani A. Doping the bismuth into the host's Cu_2ZnSnS_4 semiconductor as a novel material for thin film solar cell. Results in Physics. 2019;12:1586-1595.
23. Yang X, Qin X, Yan W, Zhang C, Zhang D. Effects of Fe and Ni Doping on the Electronic Structure and Optical Properties of Cu_2ZnSnS_4. Crystals. 2023;13(7):1082.
24. Trifiletti V, Tseberlidis G, Colombo M, Spinardi A, Luong S, Danilson M, et al. Growth and Characterization of $Cu_2Zn_{1-x}Fe_xSnS_4$ Thin Films for Photovoltaic Applications. Materials. 2020;13(6):1471.
25. Hasaneen MF, Laifi J, Alzaid M, Hadia NMA. Tunable structural, optical, and magnetic properties of Co-doped CdO nanostructures synthesized via chemical co-precipitation. Solid State Commun. 2026;412:116403.